

The Structure and Electrochemical Properties of Laser Irradiation of TiS₂ / C Composite

L.S. Yablon^{1,*}, V.V. Strelchuk², I.M. Budzulyak¹, S.I. Budzulyak²,
O.V. Morushko¹, B.I. Rachiy¹, O.M. Hemiy¹

¹ *Vasyl Stefanyk Precarpathian National University, 57, Shevchenko Str., 76018 Ivano-Frankivsk, Ukraine*

² *V.E. Lashkaryov Institute of Semiconductor Physics NAS of Ukraine, 41, Nauki Pr., 03028 Kyiv, Ukraine*

(Received 18 May 2015; published online 20 October 2015)

The optical and electrochemical properties of titanium disulfide / nanoporous carbon composite are studied for the purpose of its use in the energy storage systems. It is established that laser irradiation of the formed composite increases the specific capacity of the corresponding devices ten times and stabilizes the charge / discharge processes.

Keywords: Composite, Titan disulfide, Nanoporous carbon, Raman light scattering, Laser irradiation.

PACS numbers: 82.45.Yz, 82.47.Uv, 71.20.Tx

1. INTRODUCTION

Due to the structure and physical and chemical properties, titanium disulfide is a promising electrode material for daylight lamps and energy storage systems [1-3]. Its layer structure provides the presence of guest positions in the interlayer space which, in the context of energy and charge, can be intercalated by a relatively wide class of materials, since Van-der-Waals bonds between the layers do not prevent this. However, low electrical conductivity of TiS₂ restrains its use for the formation of electrodes of lithium power sources and electrochemical high-value capacitors. Different approaches, in particular, the use of conducting additives [4], co-intercalation technique [5], etc., are realized in order to increase the value of the electrical conductivity. It seems promising to combine the individual techniques into a single technological chain, which will give the possibility to intensify the intercalation current-formation. A composite, which was subjected to laser irradiation, with titanium disulfide and activated carbon components is produced in the proposed work. The study of the possibility to form on its basis the electrodes of hybrid electrochemical charge storage systems is performed.

2. STUDY SUBJECTS AND EXPERIMENTAL

In the experiments, we used a mechanical-chemical mixture of polycrystalline TiS₂, whose average size was equal to 50 μm, and activated carbon obtained from plant material by its hydrothermal carbonization and activation [6]. The composite was subjected to laser irradiation by YAG-laser working in the Q-switched mode with the pulse repetition frequency of $f = 20-50$ Hz for targeted modification of its physical and electrochemical properties.

A three-electrode electrochemical cell was used to study the electrochemical behavior of TiS₂/C and TiS₂/C (L) composites in aqueous electrolytes. Working electrodes were formed from the obtained composites, and platinum electrode served as an auxiliary one and silver-chlorine Ag/AgCl electrode acted as the reference one. Equilibrium electrode potential of the composite material (TiS₂/C) at room temperature with respect to the reference electrode was equal to $-0.33 - 0.28$ V. 30 % aqueous solution of

potassium hydroxide was used as the electrolyte.

The impedance spectrometer Autolab PGSTAT/FRA-2 was used to establish the nature of the response of the formed electrochemical cell to external influence.

The Raman scattering spectra of TiS₂/C and TiS₂/C (L) samples are obtained using a triple spectrometer T-64000 Horiba Jobin-Yvon equipped with confocal microscope Olimpus BX41 and thermoelectrically cooled detector. Spectra of TiS₂/C composite are recorded in the backscattering geometry at room temperature ($T = 300$ K). Ar-Kr laser line with the wavelength of $\lambda_{exc} = 514.5$ nm was used to excite the Raman spectra. Focusing of exciting radiation on the sample surface was carried out using the objective 50 × / 0.75.

3. RESULTS AND DISCUSSION

The comparative analysis of the specific capacities of the cells formed based on pure TiS₂ and TiS₂/C composite as a mechanical-chemical mixture, which contained 80 % of nanoporous carbon and 20 % of TiS₂ and was subjected to laser irradiation, is performed in this work.

In Fig. 1 we show the discharge curves for TiS₂, TiS₂/C and TiS₂/C (L), respectively, at different current values.

In order to determine the discharge capacity of the studied materials by the results of galvanostatic measurements, the following relation was used [7]:

$$C = \frac{2IA}{U_2^2 - U_1^2}, \quad (1)$$

where I is the current, A is the area under the charge/discharge curve.

Determined according to (1), specific capacity of the cell formed based on laser-irradiated TiS₂/C composite is larger compared with capacities of the initial composite and pure TiS₂ at the same current values. In particular, specific capacity for TiS₂/C (L) 10 times exceeds the capacity of the titanium disulfide cell at the current of 1 mA and 50 times – at 5 mA. Moreover, the Coulomb efficiency after 100 charge/discharge cycles for TiS₂/C (L) electrodes almost does not decrease at currents below 0.01 mA for the electrode mass, while electrodes based on TiS₂ and TiS₂/C are not able to withstand such currents.

* yablon_lyubov@ukr.net

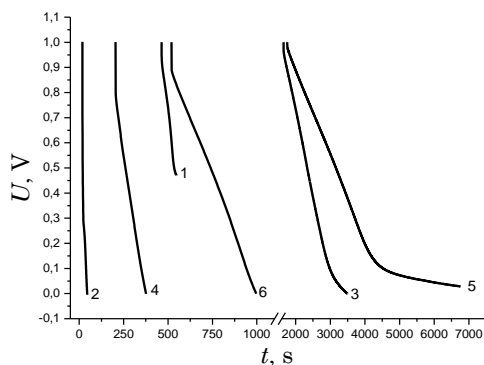


Fig. 1 – Discharge curves for the samples: TiS_2 – 1, 2; TiS_2/C – 3, 4; $\text{TiS}_2/\text{C} (L)$ – 5, 6 (1, 3, 5 – at the current of 1 mA; 2, 4, 6 – at the current of 5 mA)

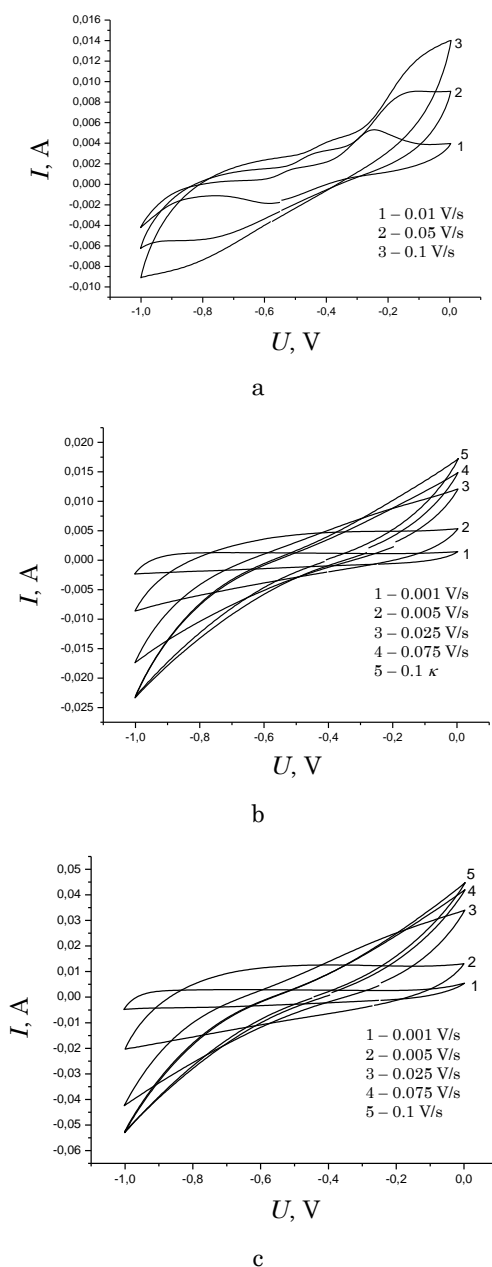


Fig. 2 – Potentiodynamic curves for: a – TiS_2 ; b – TiS_2/C and c – $\text{TiS}_2/\text{C} (L)$

Intensity of fast reverse Faradaic reactions on TiS_2 , TiS_2/C and $\text{TiS}_2/\text{C} (L)$ surfaces, respectively, in the voltage range of $-1.0-0$ was established from the analysis of the dependence of current (I) on voltage (U) at different rates of change of voltage $s = 0.001, 0.005, 0.025, 0.005, 0.1$ V/s (Fig. 2).

It is seen from Fig. 2 that with increasing scanning velocity, the shape of the dependence of I on U is changed from almost rectangular, which indicates the absence of the current change, to the prolate shape, where such a change is manifested.

The Nyquist diagrams taken for the samples TiS_2 , TiS_2/C and $\text{TiS}_2/\text{C} (L)$ and equivalent electrical circuits, which correspond to these diagrams, are shown in Fig. 3 and Fig. 4. Fitting of the elements of the equivalent electrical circuit was performed by the method proposed in [8, 9], where circuits of this type were used for modeling of the formation process on the daylight lamp electrodes of a passivating layer of finite products of the Faradaic reactions of the composite components with electrolyte. The layout of the specified circuit is not changed for all the studied composites.

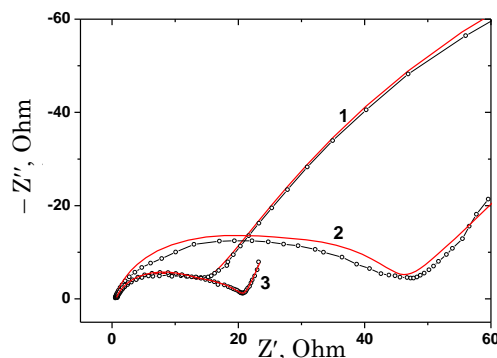


Fig. 3 – Nyquist diagrams for the electrochemical systems based on TiS_2 (1), TiS_2/C (2) and $\text{TiS}_2/\text{C} (L)$ (3) (dots are the experiment; lines are the modeling results)

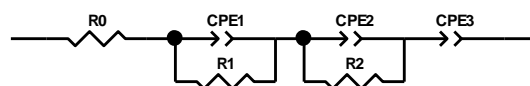


Fig. 4 – Equivalent electrical circuit used for the approximation of the Nyquist diagrams obtained for the electrochemical systems based on TiS_2 (1), TiS_2/C (2) and $\text{TiS}_2/\text{C} (L)$ (3)

To establish the reasons contributing to the increase in the specific energy and capacity characteristics of the corresponding electrochemical devices, we have obtained the Raman spectra of the initial and laser-irradiated TiS_2/C composites.

Two intense first-order phonon bands, the so-called G (“Graphitic”) and D (“Defect”) bands at ~ 1590 cm^{-1} and 1353 cm^{-1} (Fig. 5) are registered in the micro-Raman spectra of the initial and laser-irradiated TiS_2/C samples. Appearance of G and D bands is conditioned by a single-phonon process of inelastic light scattering by valence vibrations of sp^2 -bonded carbon atoms and scattering by structural defects, respectively. The relative integral intensity of the bands I_G/I_D and their full width at half maximum (FWHM) display the degree of structural disorder of the material [10]. Moreover, the phonon bands

responsible for TiS_2 are present, besides the known peaks of D and G groups for carbon, in the Raman spectra of the TiS_2/C composite subjected to laser irradiation. It is important to note that peaks of D (1343 cm^{-1}) and G (1570 cm^{-1}) groups are shifted towards the short-wave region to 1351 cm^{-1} and 1580 cm^{-1} that is conditioned by the transformation in the system of defects in TiS_2/C composite, in particular, due to the interpenetration of the composite components into pores of carbon and inter-layer positions of TiS_2 .

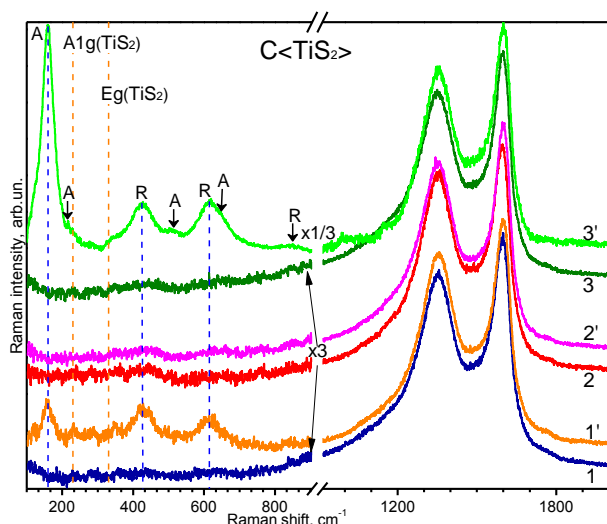


Fig. 5 – Micro-Raman spectra of the TiS_2/C composite: 1, 2, 3 (1', 2', 3') – pure mechanical mixtures (subjected to laser irradiation) at the ratio of $\text{TiS}_2 : \text{C} = 10 : 90, 20 : 80, 30 : 70$ (%), respectively. $\lambda_{\text{exc}} = 488\text{ nm}$, $T = 300\text{ K}$

In Fig. 6 we show the micro-Raman spectra in the frequency range of ($900\text{--}1850$) cm^{-1} for the initial and laser-irradiated TiS_2/C nanocomposite samples at $\text{TiS}_2 : \text{C}$ ratio (in percent, %) equal to $10 : 90$ and $30 : 70$. As seen from Fig. 6, compared with the initial sample, for laser-irradiated samples one can observe the decrease in the left arm of the D band at $\sim 1208\text{ cm}^{-1}$, whose appearance is attributed to mixing of the $\text{sp}^2\text{-sp}^3$ bonds at the periphery of crystallites, or by C–C and C=C valence vibrations of the polyene-like structures [11, 12].

The Raman spectra from TiS_2/C (L) were also recorded in the range of $200\text{--}600\text{ cm}^{-1}$ with the excitation wavelength of 633 nm . Presence of the typical peaks at 330 and 390 cm^{-1} in TiS_2 can be attributed to the A_{1g} vibrations and phonon mode [13], respectively. We should note that intensity of the peak at $\approx 330\text{ cm}^{-1}$ decreases substantially with increasing content of carbon in TiS_2 . However, peak at 390 cm^{-1} is shifted to 378 and 373 cm^{-1} in the composites of $10 : 90$ and $30 : 70$, respectively. This can be associated with possible interaction between nanoporous carbon and layered particles of TiS_2 [13].

New phonon bands corresponding to inclusions of the TiO_2 structural phase (Fig. 5, spectra 1', 3') appear in the micro-Raman spectra after laser irradiation of the TiS_2/C samples. As known, TiO_2 with the structure of anatase and rutile are the most thermodynamically stable. Structure of anatase belongs to the tetragonal crystal system and corresponds to the $D_{4h}(I4_1/amd)$ space group of symmetry. It is known from the group-theoretic analysis that six optical modes $A_{1g}(507\text{ cm}^{-1}) + 2B_{1g}(399\text{ cm}^{-1})$ and

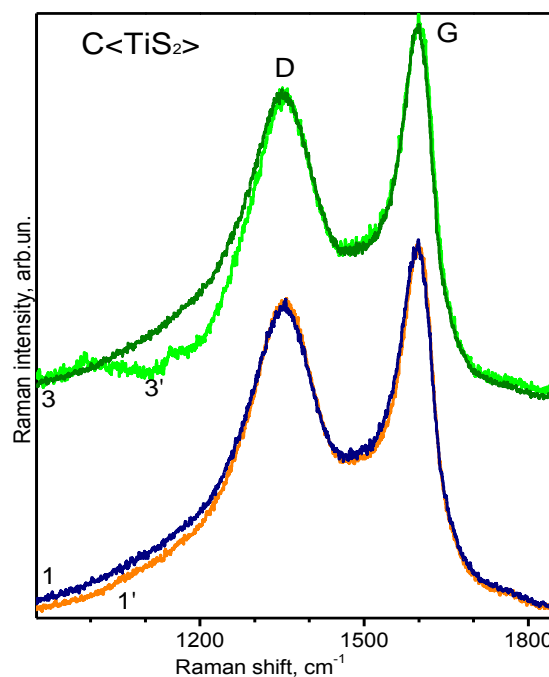


Fig. 6 – D and G bands in the micro-Raman spectra of TiS_2/C composite: 1, 3 (1', 3') – pure mechanical mixtures (subjected to laser irradiation) at the ratio of $\text{TiS}_2 : \text{C} = 10 : 90, 20 : 80, 30 : 70$ (%), respectively. $\lambda_{\text{exc}} = 488\text{ nm}$, $T = 300\text{ K}$

$519\text{ cm}^{-1} + 3E_g(144\text{ cm}^{-1}, 197\text{ cm}^{-1} \text{ and } 639\text{ cm}^{-1})$ [13] are active in the Raman spectra for this structure. Structure of rutile belongs to the tetragonal crystal system with $D_{4h}(P4_2/mnm)$ space group of symmetry. Four optical modes $A_{1g}(612\text{ cm}^{-1}) + B_{1g}(143\text{ cm}^{-1}) + B_{2g}(826\text{ cm}^{-1}) + E_g(447\text{ cm}^{-1})$ [14] are active in the Raman spectra of TiO_2 with the structure of rutile. It is seen from Fig. 5 that the phonon bands corresponding to the regions of TiO_2 inclusions with the structure of anatase and rutile (A and R, respectively) are present in the Raman spectra of the TiS_2/C composite subjected to laser irradiation. TiO_2 phonon bands are most clearly manifested in the samples with the $\text{TiS}_2 : \text{C}$ ratio (in percent, %) equal to $30 : 70$. That is, the following bands are registered: at $\sim 158\text{ cm}^{-1}$ (E_g), 215 cm^{-1} (E_g), 514 cm^{-1} ($A_{1g} : 507\text{ cm}^{-1}$ and $B_{1g} : 519\text{ cm}^{-1}$) and 648 cm^{-1} (arm A_{1g} of the rutile mode), which are typical for scattering by phonons of the anatase structural phase, and bands at $\sim 424\text{ cm}^{-1}$, 612 cm^{-1} and 841 cm^{-1} – scattering by phonons of the rutile structural phase (Fig. 5, spectrum 3'). Either only the most intense of these bands are exhibited or bands are not detected at all in other spectra.

For TiO_2 samples with mixed crystal structure, ratio of the integral intensity of E_g phonon band at 158 cm^{-1} (anatase structure) to A_{1g} phonon band at $\sim 612\text{ cm}^{-1}$ (rutile structure) is proportional to the content of these two structural phases [14]. For laser-irradiated TiS_2/C composite with $\text{TiS}_2 : \text{C}$ ratio (in percent, %), which is equal to $30 : 70$, the anatase structural phase evidently prevails compared with the rutile phase, while for the samples with $\text{TiS}_2 : \text{C}$ ratio equal to $10 : 90$, intensities of the 158 cm^{-1} (anatase) and 612 cm^{-1} (rutile) bands are almost the same that indicates a relatively equal content of both phases.

$E_g(\text{TiO}_2)$ phonon band (anatase structure) at 158 cm^{-1}

has higher value of the frequency compared with TiO₂ crystal (frequency position of the $E_g(\text{TiO}_2)$ band is equal to 144 cm⁻¹ [14]) and larger half-width ($\Gamma = 40$ cm⁻¹). Moreover, $E_g(\text{TiO}_2)$ phonon band (rutile structure) at 424 cm⁻¹ is shifted towards the low-frequency region compared with TiO₂ crystal (frequency position of the $E_g(\text{TiO}_2)$ band is equal to 447 cm⁻¹ [14]). Such changes in the frequency and half-width of the E_g phonon bands are associated with non-stoichiometry of oxygen atoms in TiO₂ crystalline matrix [15] and correspond to oxygen-depleted TiO_{2-x} regions with O / Ti = 1.89.

Thus, the local regions with the structure of rutile and anatase are formed under irradiation of the TiS₂/C composites, and the structure of the near-surface carbon nanocrystalline regions is improved.

4. CONCLUSIONS

1. It is revealed that the formed TiS₂/C composite is a promising material for the energy sources and stor-

age systems, since it has high conductivity and specific capacity, which for TiS₂/C (*L*) at the current of 1 mA 10 times exceeds the capacity of the cell based on the initial material, and at 5 mA – 50 times.

2. It is studied that the Coulomb efficiency after 100 charge/discharge cycles for TiS₂/C (*L*) electrodes almost does not decrease for currents below 0.01 A compared with electrodes based on TiS₂ and TiS₂/C, which are not able to withstand such currents.

3. It is shown that the phonon bands responsible for TiS₂ are present, besides the known peaks of the D and G groups for carbon, in the Raman spectra of the TiS₂/C composite subjected to laser irradiation. It is important to note that peaks of D (1343 cm⁻¹) and G (1570 cm⁻¹) groups are shifted towards the short-wave region to the values of 1351 cm⁻¹ and 1580 cm⁻¹, respectively, that is conditioned by the transformation in the system of defects in the TiS₂/C composite, in particular, due to the interpenetration of the composite components into carbon pores and interlayer positions of TiS₂.

REFERENCES

1. M. Stanley Whittingham, *Chem. Rev.* **104**, 4271 (2004).
2. A. Honders, J.M. der Kinderen, A.H. van Heeren et al., *Solid State Ionics* **15** No 4, 265 (1985).
3. A.L. Let, D. Mainwaing, C. Rix, P. Murugaraj, *Revue Roumaine de Chimie* **52** No 3, 235 (2007).
4. S.L. Revo, I.M. Budzulyak, B.I. Rachiy, M.M. Kuzishin, *Surf. Eng. Appl. Electrochem.* **49** No 1, 68 (2013).
5. B.K. Ostafiychuk, I.I. Hryhorchak, I.M. Budzulyak, L.S. Yablon, O.V. Morushko, *Metallofiz. Nov. Tekhnol.* **32** No 6, 749 (2010).
6. B.K. Ostafiychuk, I.M. Budzulyak, I.F. Myronyuk, I.I. Hryhorchak, *Nanomaterialy v prystroyakh heneruvannya i nakoptychennya enerhiyi* (Ivano-Frankivs'k: VDV TSIT Prykarpatskoho natsionalnoho universytetu im. V. Stefanyka: 2007) [in Ukrainian].
7. I.I. Hryhorchak, H.V. Ponedilok, *Impedansna spektroskopiya* (Lviv: Vyd-vo Lvivskoyi politekhniki: 2011) [in Ukrainian].
8. Z.B. Stoynov, B.M. Grafov, B. Savova-Stoynova, V.V. Yelkin, *Elektrokhimicheskiy impedans* (M.: Nauka: 1991).
9. P.B. Balbuena, Y. Wang, *Lithium-Ion Batteries: Solid-Electrolyte Interphase* (Imperial College Press: 2004).
10. A.C. Ferrari, J. Robertson, *Phys. Rev. B* **61**, 14095 (2000).
11. Dun Wu, Guijian Liu, Ruoyu Sun, Chen Shancheng, *Fuel* **119**, 191 (2014).
12. R. Brunetto, T. Pino, E. Dartois, A.-T. Cao, L. d'Hendecourt, G. Strazzulla, Ph. Br chignac, *Icarus* **200** No 1, 323 (2009).
13. S.V. Ovsyannikov, V.V. Shchennikov, A. Cantarero, A. Cros, A.N. Titov, *Mater. Sci. Eng. A* **462**, 422 (2007).
14. W. Ma, Z. Lu, M. Zhang, *Appl. Phys. A* **66**, 621 (1998).
15. J.C. Parker, R.W. Siegel, *Appl. Phys. Lett.* **57** No 9, 943 (1990).